Enhancing QoS Through Fluid Antenna Systems over Correlated Nakagami-m Fading Channels

Enhancing QoS Through Fluid Antenna Systems over Correlated Nakagami-m Fading Channels

Leila Tlebaldiyeva, Galymzhan Nauryzbayev, °Sultangali Arzykulov, °Ahmed Eltawil, and §#Theodoros Tsiftsis

School of Engineering and Digital Sciences, Nazarbayev University, Nur-Sultan, Z05H0K3, Kazakhstan
°CEMSE Division, King Abdullah University of Science and Technology, Thuwal, KSA 23955-6900
§Dept. of Computer Science & Telecommunications, University of Thessaly, Greece
#School of Intelligent Systems Science and Engineering, Jinan University, China
Emails: {ltlebaldiyeva, galymzhan.nauryzbayev}@nu.edu.kz, °{sultangali.arzykulov, ahmed.eltawil}@kaust.edu.sa,
§#tsiftsis@ieee.org

***Abstract*—Fluid antenna systems (FAS) enable mechanically flexible antennas that offer adaptability and flexibility for modern communication devices. In this work, we present a conceptual model for a single-antenna N-port (SANP) FAS over spatially correlated Nakagami-m fading channels and compare it with the traditional diversity schemes in terms of outage probability. The proposed FAS model switches to the best antenna port and resembles the operation of a selection combining (SC) diversity. FAS improves the quality of service (QoS) of the network through antenna port selection. The advantage of FAS is the ability to fit hundreds of antenna ports into a half-wavelength antenna size at the cost of spatial channel correlation. Simulation results demonstrate the superior outage probability performance of FAS at several tens of antenna ports compared to the traditional diversity schemes such as maximum ratio combining, equal gain combining, and SC. Moreover, the novel probability and cumulative density functions for the land mobile correlated Nakagami-m random variates are evaluated in this paper.**

***Index Terms*—Fluid antenna system (FAS), Nakagami-m fading, outage probability, single-antenna N-port (SANP) FAS.**

I. Introduction

The high quality of service (QoS) is one of the metrics in modern communication systems that motivate for new technological products and maintain revenue for telecom providers. Future communication systems require innovative fabrication solutions on the radio frequency (RF) chain components, specifically on antennas, to upgrade the performance of multiple-input multiple-output (MIMO) systems. The main limitation of MIMO antennas is the small physical size of devices to accommodate a half-wavelength separation requirement between antenna elements. For instance, IoT devices can only accommodate up to 16 antennas due to the limited physical space in millimeter wave (mmWave) frequency bands [1].

As a remedy, mechanically flexible fluid antennas have been offered for 6G communication, where a number of antenna ports are no longer an issue for mobile and IoT devices. Fluid antennas can be built on fluid materials (e.g., Mercury, Eutectic Gallium-Indium, Galinstan, etc.) and controlled by software [2]. Moreover, tunable fluid antennas may operate over a wide range of frequencies, enabling cognitive communication for IoT and mobile devices. A review on fluid antennas, including their materials, fabrication techniques, and applications, have been studied in [3]. According to [3], fluid antennas are free of mechanical deformations such as bending and stretching, which is a main physical limitation of conventional copper antennas. Materials in fluidic antennas are classified into non-conductive (acetone, ethyl acetate, etc.), partially conductive (seawater), and conductive. Moreover, fluid antennas are built on soft substrates to maintain elastic antenna properties. Moreover, the authors in [4] discussed the state-of-the-art, design configuration, advantages, and limitations of the fluid antennas.

The authors in [5] evaluated the approximate outage probability performance for single-antenna N-port (SANP) FAS over spatially correlated Rayleigh fading channels and compared its performance to the L-antenna maximal ratio-combining (MRC) receiver. According to this study, SANP FAS outperforms the L-antenna MRC receiver given that N is a large number. Moreover, the L-diversity RF chain cost and power supply could be reduced by using the FAS. The same authors studied ergodic capacity and lower bound for ergodic capacity performance as well as level crossing rate and average fade duration for the same physical FAS model in [6]. Based on this study, the FAS model was built on a small space and achieved the capacity performance of the MRC antenna system. The authors also showcased a possible architecture for the N-port FAS. Furthermore, a working prototype of a circular patch liquid microstrip antenna that uses mercury as a radiating element was reported in [7]. In addition, a 3D-printed fluidic monopole antenna system that resonates between 3.2 to 5 GHz was designed in [8]. The authors in [9] presented another working prototype for a frequency reconfigurable antenna architecture utilizing dielectric fluids.

Motivated by [5] and [6], we study the SANP equally-spaced antenna system that is exposed to correlated Nakagami-m fading channels. All antenna ports are correlated with respect to the first port by using the land mobile correlation model as in [2], [6]. One of the popular correlation models is the exponential one, which accounts for the correlation of adjacent antenna ports, as was discussed in [10]. However, this model is more applicable when multiple antenna ports are active simultaneously and correlation occurs between two adjacent antenna ports. The previous works [2], [5] and [6] studied

Rayleigh fading channel for the SANP FAS model. Although Rayleigh fading statistics simplify the analysis, it does not model line-of-sight (LOS) components between communicating nodes and only considers small-scale scattering that better suits to model the non-LOS (NLOS) signal component. According to the authors in [11] and [12], Nakagami-m fading along with analog beamforming well models the mmWave channel.

In this paper, we introduce the FAS as a method to enhance the system QoS in terms of outage probability. The key contributions of this work are listed as follows.

- We derive the joint probability density function (PDF) and cumulative density function (CDF) of the received signal at the FAS model given spatially correlated Nakagami-m fading channels. Based on it, we further evaluate the outage probability formula in a single integral form. These are novel analytical derivations as no prior work studied correlated Nakagami-m channel for the FAS model.
- Numerical analyses on the Nakagami-m fading parameter, antenna length, and signal-to-noise-ratio (SNR) threshold are investigated in terms of outage probability. It is noted that the Nakagami-m fading parameter is a major contributing factor to the outage probability performance. Furthermore, the SNR threshold has a moderate effect on the outage probability, whereas antenna length has the least contribution to the system performance.
- We also compare the outage probability performance of FAS with the conventional diversity techniques such as MRC, equal gain combining (EGC), and selection combining (SC). The FAS model demonstrated a higher performance while using several tens of antenna ports.

FAS enhances the outage probability performance of the wireless networks, thus, increases QoS experienced by users.

II. System Model

In this work, we study a system model that comprises a single-antenna transmitter (Tx) and SANP FAS-enabled receiver (Rx) built on a fluid material and connected to a single RF chain as shown in a hypothetical device in Fig. 1. A liquid metal is encapsulated into the microfluidic channel of the length d, and an antenna at location port k is treated as an ideal point antenna. We assume that FAS is able to switch to the strongest antenna port among available N ports evenly distributed over $d = \alpha\lambda$, where λ is a wavelength of the operating frequency, and α is a positive coefficient. Since antenna ports are located at close proximity to each other, the correlation phenomenon is an inevitable factor for the FAS model. Inspired by [5], we assume that $(N-1)$ ports are correlated to its first port by using the land mobile correlation model [13, Table 2.1].

We consider Nakagami-m fading for the proposed system model. The Nakagami-m distribution is a widely used model [14] that describes physical fading radio channels through the m parameter that determines the severity and existence of the direct communication link. Moreover, Nakagami-m distribution shows a good fit with the empirical data [15]. The authors in

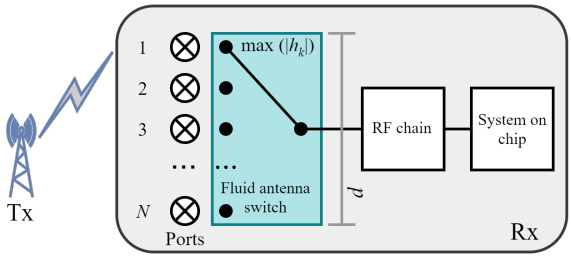

Fig. 1: A system model of SANP FAS with a antenna length, d.

[16] suggested parameterization of the correlated Nakagami-m random variables (RVs) by using the square root of a summation of m sqaured Rayleigh fading RVs to generate an envelop of the correlated Nakagami-m RV. Since N complex Gaussian RVs with zero mean and $1/2$ variance are required to implement the selection among N-port Rayleigh RVs, it will be necessary to apply $m \times N$ complex Gaussian RVs to model a correlation in Nakagami-m channels in the SANP FAS model. The channel at port $k_{|\forall k \in \mathcal{A}}$, with $\mathcal{A} = \{1, \ldots, N\}$, is modeled as $h_k = \sum_{l=1}^{m} |H_{kl}|^2$. Thus, the spatially correlated Nakagami-m fading channel at port k is parameterized as

$$H_{kl} = \sqrt{(1-\mu_k^2)}x_{kl} + \mu_k x_{0l} + j\left(\sqrt{(1-\mu_k^2)}y_{kl} + \mu_k y_{0l}\right), l = \{1, \ldots, m\}, \quad (1)$$

where x_{kl} and y_{kl} are independent Gaussian RVs with zero mean and $1/2$ variance. Moreover, the correlation coefficient, denoted by $0 < \mu_k < 1$, can be found as [13]

$$\mu_k = J_0\left(\frac{2\pi(k-1)\alpha}{N-1}\right), \quad \text{for} \quad k = \{2, \ldots, N\}, \quad (2)$$

where $J_0(\cdot)$ is the zero-order Bessel function of the first kind.

The received signal at the antenna port k is formulated as $y_k = h_k s + w$, where h_k is a Nakagami-m channel amplitude, s is a transmitted signal, and w is an additive white Gaussian noise, with zero mean and σ_w^2 variance. Note that a unity distance is assumed between Tx and Rx to focus on the main results. The PDF of the Nakagami-m RV is given by [17]

$$f_{r_k}(r_k) = \frac{2m^m r_k^{2m-1} e^{-\frac{m r_k^2}{\sigma_k^2}}}{\Gamma(m)\sigma_k^{2m}}, \quad (3)$$

where $\Gamma(\cdot)$ is the Gamma function, $m \geq 0.5$ represents the severity fading parameter, and σ_k^2 is the average channel power.

III. Outage Probability

By definition, the outage probability measures the probability that the received SNR that falls below a predefined threshold.

As mentioned before, FAS can switch to one of the strongest antenna port channel located along $d = \alpha\lambda$ length. The strongest antenna channel is denoted as $\max\{|h_1|, |h_2|, \cdots, |h_N|\}$, where $|h_1|$ is taken as a reference

port and the other $(N-1)$ ports are correlated with respect to it. Hence, outage probability for SANP FAS over spatially correlated Nakagami-m fading channel is generalized as

$$P_{\text{out}}(\gamma_{\text{th}}) = \Pr\left\{|h_1|^2 < \frac{\gamma_{\text{th}}}{\gamma}, |h_2|^2 < \frac{\gamma_{\text{th}}}{\gamma} \cdots, |h_N|^2 < \frac{\gamma_{\text{th}}}{\gamma}\right\}, \quad (4)$$

where γ_{th} is the SNR-associated threshold, γ is the average received SNR estimated by $\gamma = \frac{\mathbb{E}\{|h_k|^2\}\mathbb{E}\{|s|^2\}}{\sigma_w^2}$, and $\mathbb{E}\{\cdot\}$ stands for the expectation operator.

To evaluate the outage probability, we need to derive the PDF and CDF of joint Nakagami-m RVs, which are calculated in Proposition 2 and Theorem 1, respectively. It is essential to obtain the PDF of two joint Nakagami-m variates that are spatially correlated with respect to the port 1 to find the general PDF formula for N correlated Nakagami-m variates. Proposition 1 evaluates the conditional PDF of two jointly distributed Nakagami-m RVs.

Proposition 1: Let $|h_1|$ and $|h_2|$ be non-negative Nakagami-m RVs. A conditional probability of $|h_2|$ on $|h_1|$ is given by

$$f_{|h_2|\big||h_1|}(r_2|r_1) = \frac{2m r_1^{1-m} r_2^m \sigma_1^{m-1} e^{-\frac{m}{1-\mu_2}\frac{r_2^2}{\sigma_2^2} e^{-\frac{\mu_2^2 m}{1-\mu_2}\frac{r_1^2}{\sigma_1^2}}}}{\sigma_2^{m+1}(1-\mu_2^2)\mu_2^{m-1}} \times I_{m-1}\left[\frac{2m\mu_2 r_1 r_2}{(1-\mu_2^2)\sigma_1\sigma_2}\right], \quad (5)$$

where $I_{m-1}(\cdot)$ is the $(m-1)$th order modified Bessel function of the first kind, μ_2 is the correlation coefficient of the second port, and $\sigma^2_{k|k\in\{1,2\}}$ is the average signal power.

Proof: The proof is presented in Appendix A. ■

By making use of *Proposition* 1, the joint PDF of N correlated Nakagami-m RVs is evaluated as below.

Proposition 2: The joint PDF of N spatially correlated $|h_{k|k\in\mathcal{A}}|$ Nakagami-m RVs is computed as

$$f_{|h_1|,\cdots,|h_N|}(r_1,\cdots,r_N) = \frac{2r_1^{2m-1}m^m}{\Gamma(m)\sigma_1^{2m}} e^{-\frac{r_1^2 m}{\sigma_1^2}} \times \prod_{k=2}^{N} \frac{2m r_1^{1-m} r_k^m \sigma_1^{m-1}}{\sigma_k^{m+1}(1-\mu_k^2)\mu_k^{m-1}} e^{-\frac{m\sigma_1^2 r_k^2 + m\sigma_k^2 r_1^2 \mu_k^2}{\sigma_1^2\sigma_k^2(1-\mu_k^2)}} \times I_{m-1}\left[\frac{2m\mu_k r_1 r_k}{\sigma_1\sigma_k(1-\mu_k^2)}\right]. \quad (6)$$

Proof: The proof is given in Appendix B. ■

The next corollary estimates the joint PDF for the N uncorrelated Nakagami-m fading channels.

Corollary 1: Now, we will consider a case with no correlation between channels, i.e., $\mu_k = 0$. However, a simple substitution of $\mu_k = 0$ into (6) will lead to an undefined result because of the "0/0" term. Therefore, we proceed by expanding the modified Bessel function term in terms of its series representation as in [18, (8.445)] and get the following identity for limiting behavior

$$\lim_{\mu_k\to 0} \frac{1}{\mu_k^{m-1}} I_{m-1}\left[\frac{2m\mu_k r_1 r_k}{\sigma_1\sigma_k(1-\mu_k^2)}\right] = \frac{1}{\Gamma(m)}\left(\frac{m r_1 r_k}{\sigma_1\sigma_k}\right)^{m-1}. \quad (7)$$

By utilizing (7) and taking the limit in (6), one can obtain

$$f_{|h_1|,\cdots,|h_N|}(r_1,r_2,\cdots,r_N) = \prod_{k=1}^{N} \frac{2m^m r_k^{m-1}}{\Gamma(m)\sigma_k^{2m}} e^{-\frac{r_k^2 m}{\sigma_k^2}}. \quad (8)$$

This means that if there is no correlation; thus, the combined PDF equals the product of individual PDFs obtained using (3).

The CDF of N jointly distributed Nakagami-m RVs is assessed in the next theorem.

Theorem 1: The joint CDF of N correlated Nakagami-m RVs is calculated as

$$F_{|h_1|,|h_2|,\cdots,|h_N|}(r_1,r_2,\cdots,r_N) = \frac{2m^m}{\Gamma(m)\sigma_1^{2m}} \int_0^{R_1} r_1^{2m-1} e^{-\frac{m r_1^2}{\sigma_1^2}} \times \prod_{k=2}^{N}\left[1 - Q_{\text{m}}\left(\sqrt{\frac{2m\mu_k^2 r_1^2}{\sigma_1^2(1-\mu_k^2)}}, \sqrt{\frac{2mR_k^2}{\sigma_k^2(1-\mu_k^2)}}\right)\right] \mathrm{d}r_1, \quad (9)$$

where Q_{m} is the Marcum Q-function.

Proof: The proof is relegated in Appendix C. ■

The following key theorem delivers the outage probability expression for the system under study.

Theorem 2: Suppose $|h_{k|k\in\mathcal{A}}|$ are correlated Nakagami-m RVs. The outage probability for SANP FAS is evaluated as

$$P_{\text{out}}(\gamma_{\text{th}}) = \frac{2m^m}{\Gamma(m)\sigma_1^{2m}} \int_0^{\sqrt{\frac{\gamma_{\text{th}}}{\gamma}}} r_1^{2m-1} e^{-\frac{m r_1^2}{\sigma_1^2}} \times \prod_{k=2}^{N}\left(1 - Q_{\text{m}}\left(\sqrt{\frac{2m\mu_k^2 r_1^2}{\sigma_1^2(1-\mu_k^2)}}, \sqrt{\frac{2m\gamma_{\text{th}}}{\sigma_k^2(1-\mu_k^2)\gamma}}\right)\right) \mathrm{d}r_1. \quad (10)$$

Proof: By setting $R_1 = R_2 = \cdots = R_N = \sqrt{\frac{\gamma_{th}}{\gamma}}$ into the CDF given in (9), we get the outage probability formula. ■

IV. Numerical Results and Discussion

This section is devoted to study the outage probability performance of the proposed system model for different fading, threshold, and antenna length parameters. As a rule of thumb, an improvement of outage probability directly enhances the network QoS. In Fig. 2, the performance of 100-port FAS is studied for the fading parameters $m = \{1, 2, 4, 6\}$ and antenna sizes $\alpha = \{1, 5\}$ at the threshold $\gamma_{\text{th}} = 5$ dB. First, it is observed that a five-times increase in antenna size has resulted in the improved outage performance. For instance, when $m = 4$, $N = 10$, a curve with $\alpha = 1$ reaches $P_{\text{out}} = 1.2 \times 10^{-4}$, whereas a curve with $\alpha = 5$ attains $P_{\text{out}} = 2.7 \times 10^{-5}$. Secondly, this figure demonstrates a crucial impact of fading parameters on the outage probability. The NLOS and LOS cases are modeled by setting $m = 1$ and $m = \{4, 6\}$, respectively. To attain $P_{\text{out}} = 0.05$ with $m = \{1, 2, 4, 6\}$ channel models, FAS requires $N = \{90, 18, 3, 2\}$ ports, correspondingly. Hence, FAS at $m = \{4, 6\}$ would require 30- and 45-times less ports compared to the NLOS one.

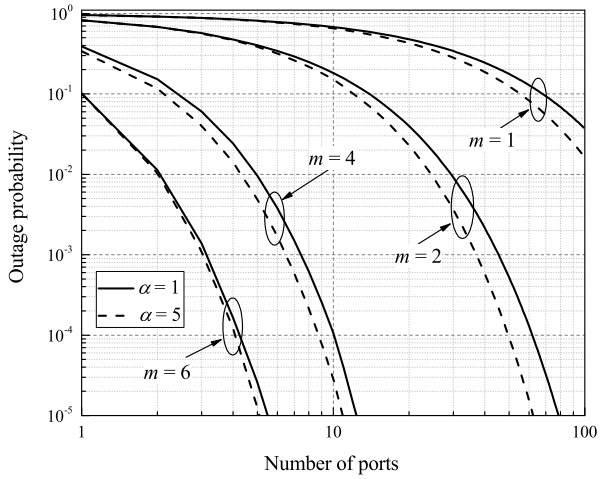

Fig. 2: Outage probability, when $m = \{1, 2, 4, 6\}$, $\alpha = \{1, 5\}$, and $\gamma_{\rm th} = 5$ dB.

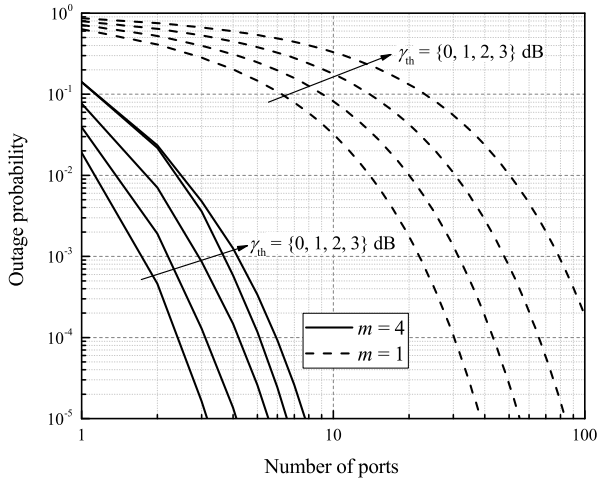

Fig. 3: Outage probability, when $\gamma_{\rm th} = \{0, 1, 2, 3\}$ dB, $\alpha = 0.5$, and $m = \{1, 4\}$.

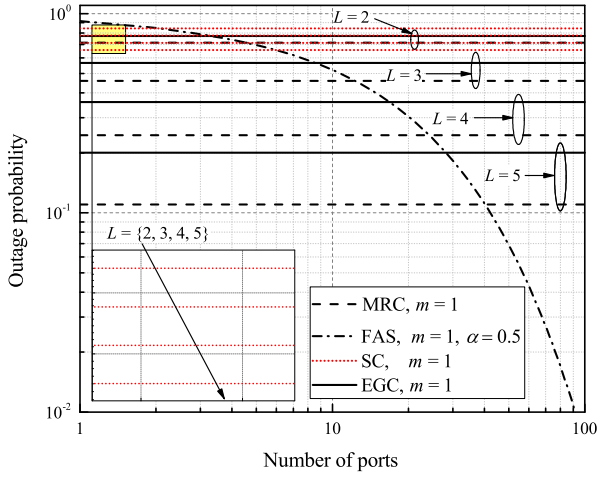

Fig. 4: Outage probability, when $\gamma_{\rm th} = 53$ dB, $\alpha = 0.5$, $m = 1$, and MRC/EGC/SC receivers with $L = \{2, 3, 4, 5\}$.

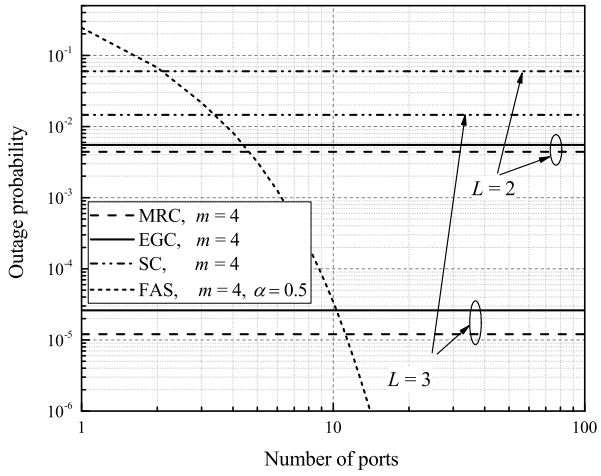

Fig. 5: Outage probability, when $\gamma_{\rm th} = 5$ dB, $\alpha = 0.5$, $m = 4$, and MRC/EGC/SC receivers with $L = \{2, 3, 4, 5\}$.

In Fig. 3, we study how the SNR threshold values $\gamma_{th} = \{0, 1, 2, 3\}$ dB affect the outage probability performance at the LOS/NLOS channel cases while FAS size is $\alpha = 0.5$. As expected, lower SNR threshold values produce lower outage probabilities and thus improve the system performance for both LOS/NLOS cases. For example, at $m = 1$ and $N = 30$, we record $P_{\rm out} = \{9 \times 10^{-5}, 0.001, 0.01, 0.05\}$ for the corresponding $\gamma_{\rm th} = \{0, 1, 2, 3\}$ dB. For each dB unit increase, there is, at least, five-times outage probability performance degradation. Moreover, we observe a significant outage performance difference between the LOS and NLOS cases at the same SNR thresholds. For instance, at $\gamma_{\rm th} = 1$ dB and $N = 3$, the $m = 4$ curve results in $P_{\rm out} = 10^{-4}$, and the $m = 1$ curve shows $P_{\rm out} = 0.4$.

In Figs. 4-5, we analyze how FAS is compatible with the conventional MRC [19, (3)], EGC [20, (3)], and SC [21] diversity techniques under the LOS/NLOS channel conditions. More precisely, in Fig. 4, we study FAS with the size $\alpha = 0.5$ at $m = 1$ and $\gamma_{\rm th} = 4$ dB. The dashed, solid and dash-dotted lines represent the MRC, EGC and SC receivers, respectively, with $L = \{2, 3, 4, 5\}$ branches that define the diversity order. This figure illustrates how many ports are necessary for the FAS scenario to outperform the conventional diversity methods. Thus, FAS outperforms the order-2 MRC and EGC diversity schemes, when the system is deployed with $N \geq 5$ and $N \geq 3$ ports, respectively. Likewise, FAS surpasses the $L = 5$-order MRC and EGC curves, when the number of ports is above $N = 40$ and $N = 28$, accordingly. A complete comparison table between FAS and the conventional diversity receivers is presented in Table I.

In Fig. 5, we analyze the communication at the LOS scenario, when $m = 4$, $\gamma_{\rm th} = 4$, and $\alpha = 0.5$. From this figure, FAS with four ports excels the $L = 2$- order MRC and EGC schemes. Likewise, FAS outperforms the SC scheme, when the system is equipped with, at least, two ports. Similarly, FAS beats the $L = 3$-order MRC, EGC, SC scenarios, when $N > 11$,

Table I: The amount of FAS ports required to outperform the MRC/EGC/SC techniques.

Order of diversity	Qty per MRC/EGC/SC
$L = 2$	5/3/2
$L = 3$	11/8/3
$L = 4$	24/17/5
$L = 5$	40/28/6

$N > 10$, and $N > 2$, respectively. It is pertinent to note that FAS (equipped with dozens of ports evenly distributed over half-wavelength antenna space) is able to achieve a better outage performance than its three counterparts at the LOS/NLOS scenarios. Moreover, note that the MRC and EGC diversity schemes require channel state information and L-order RF-chain components compared to FAS, which needs only a single RF chain as the SC scheme does. Every additional diversity order for MRC and EGC requires an extra cost of RF chains. On the other hand, SC demonstrates the worst performance compared to the other diversity schemes and FAS.

Fig. 6 illustrates the outage performance for the MRC and FAS scenarios, with different transmit SNR values at the threshold $\gamma_{\text{th}} = 10$ dB and $m = 2$. We consider MRC, with $L = \{2, 3, 4\}$, and FAS, with $N = \{100, 200, 300, 500\}$ antenna ports spread over the space defined by $\alpha = \{1, 1.5\}$. We assume that MRC is characterized by a $\lambda/2$ antenna separation maintained between the two neighbouring antennas. Therefore, we have selected the proportional FAS antenna sizes of $\alpha = \{1, 1.5\}$ that directly correspond to MRC with $L = \{3, 4\}$. From this plot, $N = 500$-port FAS outperforms the $L = 2$ MRC above 4.12 dB and the $L = 3$ MRC above 5.14 dB of transmit SNR, correspondingly. However, the FAS performance is worse than the one of MRC with $L = 4$. There is a notable outage metric improvement when the antenna port size rises from 100 to 500 antenna ports. For instance, at $P_{\text{out}} = 0.001$, FAS with $\alpha = 1.5$ on average requires at least 0.54 dB SNR for every 100 ports. Next, the antenna size has demonstrated a minor influence on the outage probability performance as opposed to the number of antenna ports.

V. Conclusion

Traditional conductive antennas often are not suitable for certain applications that requires flexibility and reconfigurability of electromagnetic performance. FAS offers many advantages as low cost, small size, flexibility, and high performance. In this work, we derived the outage probability performance of SANP FAS over spatially correlated Nakagami-m fading channels. Previous works have not analyzed correlated Nakagami-m fading channels for the proposed system model. The FAS model with the order of tens ports demonstrated a higher performance than the MRC and EGC diversity schemes of the $L = \{2, 3\}$ order. Moreover, FAS requires less than ten ports to achieve the performance of the SC scheme. Thus, it is possible to increase the network QoS by increasing the number of antenna ports. The future work aims to build a hardware prototype of FAS to justify its advantage over traditional antenna diversity schemes.

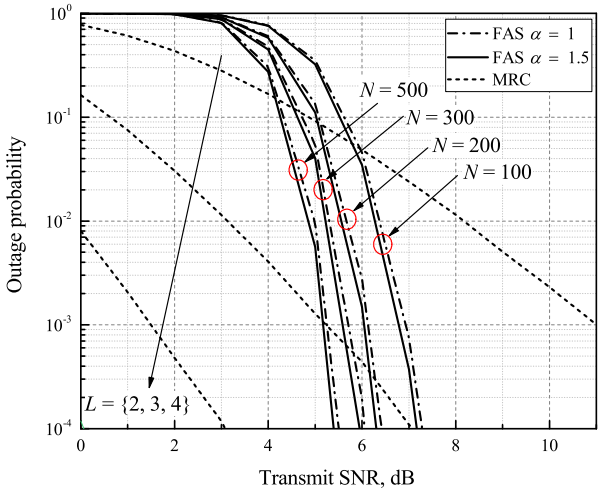

Fig. 6: Outage probability, when $\gamma_{\text{th}} = 10$ dB, $\alpha = \{1, 1.5\}$, $N = \{100, 200, 300, 500\}$, $m = 2$, and MRC receivers with $L = \{2, 3, 4\}$.

Appendix A
Proof of Proposition 1.

The PDF $f_{|h_2|\big||h_1|}(r_2|r_1)$ of the two-port FAS conditioned on port 1 is computed by taking a ratio of the joint probability of two RVs $f_{|h_1|,|h_2|}(r_1, r_2)$ over the PDF of $|h_1|$ as

$$f_{|h_2|\big||h_1|}(r_2|r_1) = \frac{f_{|h_1|,|h_2|}(r_1, r_2)}{f_{|h_1|}(r_1)}, \tag{A.1}$$

where the joint PDF of two correlated Nakagami-m variates is given in [13, (6.1)] as

$$\begin{aligned} f_{|h_1|,|h_2|}(r_1, r_2) =& \frac{4m^{m+1}(r_1 r_2)^m e^{-\frac{m}{1-\mu_2^2}\left(\frac{r_1^2}{\sigma_1^2}+\frac{r_2^2}{\sigma_2^2}\right)}}{\Gamma(m)\sigma_1^2\sigma_2^2(1-\mu_2^2)(\sigma_1\sigma_2\mu_2)^{m-1}} \\ & \times I_{m-1}\left(\frac{2m\mu_2 r_1 r_2}{(1-\mu_2^2)\sigma_1\sigma_2}\right). \end{aligned} \tag{A.2}$$

By taking the ratio of (A.2) and (3), the conditional probability for spatially correlated two ports is calculated in (5).

Appendix B
Proof of Proposition 2.

First, the PDF of multiple Nakagami ports conditioned on port 1 is the product of terms in (5)

$$\begin{aligned} f_{|h_2|,\cdots,|h_M|\big||h_1|}(r_2, \cdots, r_M|r_1) &= \prod_{k=2}^{N} f_{|h_k|\big||h_1|}(r_k|r_1) \\ &= \prod_{k=2}^{N} \frac{2m r_1^{1-m} r_k^m \sigma_1^{m-1} e^{-\frac{m}{1-\mu_k}\frac{r_k^2}{\sigma_k^2}} e^{\frac{m}{1-\mu_k^2}\frac{r_k^2}{\sigma_k^2}}}{\sigma_k^2(1-\mu_k^2)(\sigma_1\sigma_k\mu_k)^{m-1}} \\ &\quad \times I_{m-1}\left[\frac{2m\mu_k r_1 r_k}{(1-\mu_k^2)\sigma_1\sigma_k}\right]. \end{aligned} \tag{B.1}$$

Next, by multiplying (3) and (B.1), we obtain the joint PDF for N Nakagami-m variates in (6).

APPENDIX C
PROOF OF THEOREM 1.

To find the CDF, the following integral needs to be evaluated

$$\bar{F} = F_{|h_1|,|h_2|,\ldots,|h_N|}(r_1, r_2, \ldots, r_N) = \int_0^{R_1} \cdots \int_0^{R_N} f_{|h_1|,\cdots,|h_N|}(r_1, \ldots, r_N) \mathrm{d}r_1 \cdots \mathrm{d}r_N. \quad \text{(C.1)}$$

By using [18, (8.445)], substituting (6) into (C.1), and performing some algebraic simplifications, we get

$$\begin{aligned}\bar{F} = \frac{1}{\Gamma(m)} \left(\prod_{\substack{k=1 \\ \mu_1=0}}^{N} \frac{2m^m}{(1-\mu_k^2)^m \sigma_k^{2m}} \right) \\ \times \int_0^{R_1} r_1^{2m-1} e^{-\left(\frac{m}{\sigma_1^2} + \sum_{k=2}^{N} \frac{m\mu_k^2}{\sigma_1^2(1-\mu_k^2)}\right) r_1^2} \\ \times \left[\prod_{k=2}^{N} \sum_{i_k=0}^{\infty} \frac{1}{i_k! \Gamma(m+i_k)} \left(\frac{m\mu_k r_1}{\sigma_1 \sigma_k (1-\mu_k^2)} \right)^{2i_k} \right. \\ \left. \times \int_0^{R_k} r_k^{2m-1+2i_k} e^{-\frac{m}{\sigma_k^2(1-\mu_k^2)} r_k^2} dr_k \right] \mathrm{d}r_1. \end{aligned} \quad \text{(C.2)}$$

Using [18, (3.381.1)] and applying the change of variables, the internal integral in terms of r_k can be evaluated as

$$\begin{aligned}\int_0^{R_k} r_k^{2m-1+2i_k} e^{-\frac{m}{\sigma_k^2(1-\mu_k^2)} r_k^2} \mathrm{d}r_k \\ = \frac{1}{2} \left(\frac{m}{\sigma_k^2(1-\mu_k^2)} \right)^{-m-i_k} \gamma\left(m + i_k, \frac{mR_k^2}{\sigma_k^2(1-\mu_k^2)} \right), \end{aligned} \quad \text{(C.3)}$$

where $\gamma(\cdot,\cdot)$ is the lower incomplete gamma function. If (C.3) is substituted into (C.2) and then some algebraic manipulations are performed, we get

$$\begin{aligned}\bar{F} = \frac{2m^m}{\Gamma(m)\sigma_1^{2m}} \int_0^{R_1} r_1^{2m-1} e^{-\left(\frac{m}{\sigma_1^2} + \sum_{k=2}^{N} \frac{m\mu_k^2}{\sigma_1^2(1-\mu_k^2)}\right) r_1^2} \\ \times \left[\prod_{k=2}^{N} \sum_{i_k=0}^{\infty} \frac{r_1^{2i_k}}{i_k! \Gamma(m+i_k)} \left(\frac{m\mu_k^2}{\sigma_1(1-\mu_k^2)} \right)^{i_k} \right. \\ \left. \times \gamma(m+i_k, \frac{mR_k^2}{\sigma_k^2(1-\mu_k^2)}) \right] \mathrm{d}r_1. \end{aligned} \quad \text{(C.4)}$$

We note that the integral in (C.4) can not be evaluated due to the presense of a sum inside the product, which also contains the integration variable r_1. By using [18, (8.356.3)] and the definition of the Marqum Q-function

$$Q_{\mathrm{m}}(\alpha, \beta) = e^{-\frac{\alpha^2}{2}} \sum_{i_k=0}^{\infty} \frac{1}{i_k!} \left(\frac{\alpha^2}{2} \right)^{i_k} \frac{\Gamma(m+i_k, \beta^2/2)}{\Gamma(m+i_k)}, \quad \text{(C.5)}$$

where in our case $\alpha^2 = \frac{2m\mu_k^2 r_1^2}{\sigma_1^2(1-\mu_k^2)}$ and $\beta^2 = \frac{2mR_k^2}{\sigma_k^2(1-\mu_k^2)}$, we rewrite (C.4) as the final CDF expression shown in (9).

Remark: The validity of (9) or (C.4) can be checked as follows. Let us consider two extreme cases.

Case 1: we assume that all integration limits are defined as $R_1 = \ldots = R_N = \infty$. Their substitution into (C.4) precisely results in $\bar{F} = 1$.

Case 2: we assume that all integration limits are zero, i.e., $R_1 = \ldots = R_N = 0$; this leads $\bar{F} = 0$. Therefore, both outputs support the domain of the outage metric.

REFERENCES

[1] J. G. Andrews *et al.*, "Modeling and Analyzing Millimeter Wave Cellular Systems," *IEEE Trans. Commun.,* vol. 65, no. 1, pp. 403-430, Jan. 2017.

[2] K.-K. Wong *et al.*, "Fluid Antenna System for 6G: When Bruce Lee Inspires Wireless Communications," *Electron. Lett.,* vol. 56, no. 24, pp. 1288-1290, Nov. 2020.

[3] K. Paracha *et al.*, "Liquid Metal Antennas: Materials, Fabrication and Applications," *Sens.,* vol. 20, no. 1, p. 177, 2019.

[4] E. Motovilova and S. Huang, "A Review on Reconfigurable Liquid Dielectric Antennas," *Materials*, vol. 13, no. 8, p. 1863, 2020. Available: 10.3390/ma13081863.

[5] K.-K. Wong *et al.*, "Fluid Antenna Systems," *IEEE Trans. Wirel. Commun.*, vol. 20, no. 3, pp. 1950-1962, Mar. 2021.

[6] K.-K. Wong *et al.*, "Performance Limits of Fluid Antenna Systems," *IEEE Commun. Lett.*, vol. 24, no. 11, pp. 2469-2472, Nov. 2020.

[7] Y. Kosta and S. Kosta, "Liquid Antenna Systems," *IEEE Antennas Propag. Soc. Symp.*, Monterey, CA, USA, 2004, pp. 2392-2395.

[8] C. Borda-Fortuny *et al.*, "Low-Cost 3D-Printed Coupling-Fed Frequency Agile Fluidic Monopole Antenna System," *IEEE Access*, vol. 7, pp. 95058-95064, 2019.

[9] M. Konca and P. A. Warr, "A Frequency-Reconfigurable Antenna Architecture Using Dielectric Fluids," *IEEE Trans. Antennas Propag.*, vol. 63, no. 12, pp. 5280-5286, Dec. 2015.

[10] N. Zlatanov, Z. Hadzi-Velkov, and G. Karagiannidis, "An Efficient Approximation to the Correlated Nakagami-m Sums and its Application in Equal Gain Diversity Receivers", *IEEE Trans. Wirel. Commun.*, vol. 9, no. 1, pp. 302-310, Jan. 2010.

[11] S. Kusaladharma, W. Zhu, and W. Ajib, "Outage Performance and Average Rate for Large-Scale Millimeter-Wave NOMA Networks," *IEEE Trans. Wirel. Commun.*, vol. 19, no. 2, pp. 1280-1291, Feb. 2020.

[12] T. Bai and R. W. Heath, "Coverage and Rate Analysis for Millimeter-wave Cellular Networks," *IEEE Trans. Wirel. Commun.*, vol. 14, no. 2, pp. 1100-1114, Feb. 2015.

[13] M. K. Simon and M. S. Alouini, *Digital Communications over Fading Channels*, 2nd ed. John Wiley I & Sons, 2005.

[14] S. Ikki and M. H. Ahmed, "Performance Analysis of Cooperative Diversity Wireless Networks over Nakagami-m Fading Channel," *IEEE Commun. Lett.,* vol. 11, no. 4, pp. 334-336, Apr. 2007.

[15] H. Suzuki, "A Statistical Model for Urban Multipath," *IEEE Trans. Commun.*, vol. 25, no. 7, pp. 673–680, Jul. 1977.

[16] Y. Chen and C. Tellambura, "Distribution functions of selection combiner output in equally correlated Rayleigh, Rician, and Nakagami-m fading channels," *IEEE Trans. Commun.*, vol. 52, no. 11, pp. 1948-1956, Nov. 2004.

[17] G. Nauryzbayev *et al.*, "Performance of Cooperative Underlay CR-NOMA Networks over Nakgami-m Channels," *IEEE Int. Conf. Commun. Workshops (ICC WKSH)*, pp. 1-6, Kansas City, USA, May 2018.

[18] I. S. Gradshteyn and I. M. Ryzhik, *Table of integrals, series, and products.* Elsevier/Academic Press, Amsterdam, 7th ed., 2007.

[19] Y. G. Kim and N. C. Beaulieu, "New Results on Maximal Ratio Combining in Nakagami-m Fading Channels," *IEEE Int. Conf. Commun. (ICC),* Ottawa, Canada, pp. 4761-4765, Jun. 2012.

[20] A. Annamalai, C. Tellambura, and V. K. Bhargava, "Exact Evaluation of Maximal-Ratio and Equal-Gain Diversity Receivers for M-ary QAM on Nakagami Fading Channels," *IEEE Trans. Commun.*, vol. 47, no. 9, pp. 1335-1344, Sept. 1999.

[21] O. C. Ugweje and V. A. Aalo, "Performance of Selection Diversity System in Correlated Nakagami Fading," *IEEE Veh. Technol. Conf.,* Phoenix, USA, May 1997, pp. 1488-1492.